

Mechanism of the incommensurate phase in lead oxide α -PbO

D. Le Bellac

Laboratoire Léon Brillouin, CEA, CNRS, Centre d'Etudes de Saclay, 91191 Gif-sur-Yvette Cedex, France

J. M. Kiat*

*Laboratoire de Chimie-Physique du Solide, URA 453, au CNRS, Ecole Centrale, 92295 Chatenay-Malabry, France
and Laboratoire Léon Brillouin, CEA, CNRS, Centre d'Etudes de Saclay, 91191 Gif-sur-Yvette Cedex, France*

P. Garnier

Laboratoire de Chimie-Physique du Solide, URA 453, au CNRS, Ecole Centrale, 92295 Chatenay-Malabry, France

H. Moudden

Laboratoire Léon Brillouin, CEA, CNRS, Centre d'Etudes de Saclay, 91191 Gif-sur-Yvette Cedex, France

Ph. Sciau

Laboratoire de Chimie-Physique du Solide, URA 453, au CNRS, Ecole Centrale, 92295 Chatenay-Malabry, France

P. A. Buffat

Institut Départemental de Lausanne, Ecole Polytechnique Fédérale de Lausanne, Lausanne, Switzerland

G. André

Laboratoire Léon Brillouin, CEA, CNRS, Centre d'Etudes de Saclay, 91191 Gif-sur-Yvette Cedex, France

(Received 23 February 1995)

We report detailed studies of the incommensurate phase of lead oxide α -PbO using neutron and x-ray scattering as well as electron-diffraction techniques. Comparison of the structural evolution of α -PbO with those of two isostructural compounds, $\text{Pb}_{1-x}\text{Ti}_x\text{O}$ ($4.5 < x < 8$ mol %) and tin oxide SnO, has been made. The experimental results clearly suggest that the incommensurate phase observed in α -PbO is of the displacive type, induced by the softening of a lattice phonon mode. Using a simple ionic approximation we have studied the localization of the lone pairs inside the structures of the three isotopic compounds using a simple model of competing Coulomb interactions which leads to unstable positions of Pb^{2+} and O^{2-} ions in the average structure. The stability of the incommensurate phase down to the lowest temperatures seems to be favored by the frustration arising from the next-nearest-neighbor Coulomb interaction.

I. INTRODUCTION

Lead oxide PbO exists at room temperature in two polymorphic forms: (red) litharge usually called α -PbO, with a tetragonal cell ($P4/nmm$) and (yellow) massicot β -PbO, with an orthorhombic cell ($Pbma$). Both compounds have very simple structures which are characterized by a similar packing of the lead atoms; a transformation between both phases is easily obtained at room temperature by grinding or by the presence of water. The physical properties of these compounds are well known and have long been of industrial interest, particularly because of their semiconductor and photoconductor properties. Recently there has been a renewal of interest in the study of this compound as two new phases have been evidenced: an orthorhombic phase ($Pm2_1n$) at room temperature under high pressure¹ (above 0.7 GPa) and an incommensurate phase (P_{-1-11}^{C2mb}) at ambient pressure and low temperature² (below $T_1 \approx 208$ K); moreover chemical oscillations at the $\alpha \leftrightarrow \beta$ transition have been detected with possible chaotic states.³

In this paper we are interested in the α -PbO form and particularly in its low-temperature structural evolution. At

room temperature the structure is a stacking of regular square pyramids (Fig. 1) with the Pb^{II} ions located at the apex of four basal oxygen atoms. These $[\text{PbO}_4]$ polyhedra are connected to form layers orthogonal to the tetragonal c axis. The electronic lone pairs of the Pb^{2+} ions extend parallel to the fourfold axis and occupy the large interlayer distance, with a volumic occupancy equivalent to that of an oxygen atom.⁴

We have already reported a low-temperature modulation of this structure:² indeed below about 208 K α -PbO transforms into an incommensurate ferroelastic phase with an orthorhombic average structure. A preliminary structural analysis of this phase reveals that both Pb and O atoms are displaced from the average atomic positions which remain very close to those determined from the basic nonmodulated phase.⁵ This transformation exhibits unusual features: (i) very strong precursor effects in the form of diffuse scattering are observed far above the transition temperature, (ii) no temperature evolution of the incommensurate parameter [$\delta = 0.185(\mathbf{a}_t^* + \mathbf{b}_t^*) = 0.370\mathbf{b}_0^*$] and no lock-in transition down to 8 K are observed.² Besides, we have suggested that the electronic lone pairs of the Pb^{II} atoms could play an important role in the mechanism of the phase transition. One

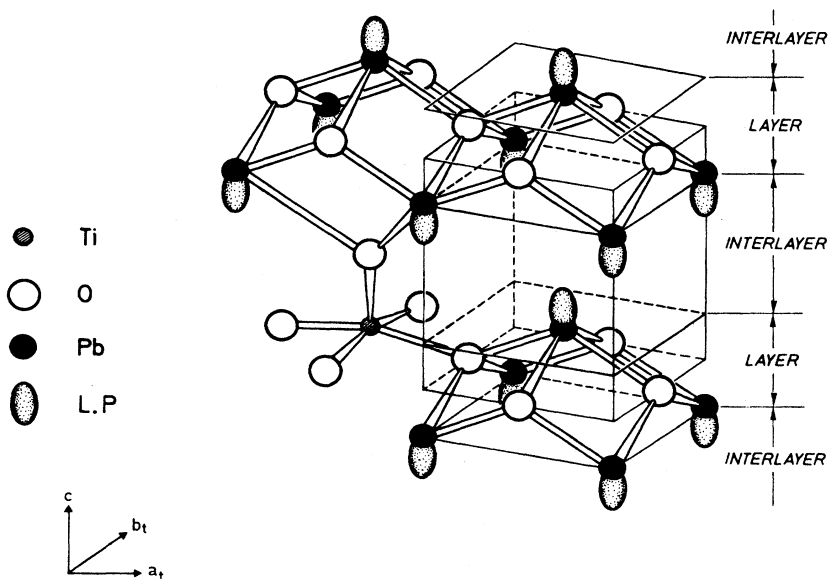


FIG. 1. Room-temperature tetragonal structure of α -PbO and $\text{PbO}_{(1-x)}(\text{TiO})_x\text{O}$.

great experimental difficulty for the study of this compound is the impossibility to grow large single crystals. Indeed up to now, as far as the pure α -PbO is concerned, only platelike crystals with an area of about 1 mm^2 and a thickness smaller than some $10 \mu\text{m}$ could be grown. On the other hand, introduction of titanium oxide TiO_2 in the structure of lead oxide α -PbO was reported to be one way to facilitate the synthesis of large single crystals.⁶ In this case solid solutions $\text{Pb}_{1-x}(\text{TiO})_x\text{O}$ with x ranging between 4.5–8 mol % can be obtained with the litharge structure. From the structural point of view we have shown⁷ that a TiO_2 group (with Ti^{IV}) can be substituted for a PbOL group, L being the associated electronic lone pair, the extra oxygen atom filling the volume of this lone pair (Fig. 1). However in this case the incommensurate phase is suppressed (see below). The absence of the incommensurate phase transition is also shown in the isostructural tin oxide SnO which remains tetragonal down to 2 K.⁸ Comparison of the structural evolution of α -PbO with that of these two isostructural compounds is one of the clues for the understanding of the mechanism of the phase transition, as we will discuss.

We have studied these three isostructural compounds by using a combination of x-ray and neutron scattering on powdered samples and electron diffraction on small single crystals. The results are supported by a model calculation that we have developed to study the ground-state energy and configuration of the electronic lone pairs in periodically ordered structures.¹⁰ The aim of this paper is to present these experimental results and the model calculations in order to shed some light on the mechanism of the phase transition. The stability of the incommensurate phase in the lead or tin oxides is discussed in terms of the competing short- and long-range Coulomb interaction of the lone pairs.

II. EXPERIMENTAL

Well crystallized powdered samples of α -PbO were prepared by thermal decomposition of lead dioxide β - PbO_2 (Merck for analysis) in air at 855 K for 2 h. Commercial SnO

powder was used (Merck for analysis). $\text{Pb}_{1-x}(\text{TiO})_x\text{O}$ compounds with $x=0.06$ were obtained by solid-state reaction between β -PbO and TiO_2 at 975 K for 2 days. Small single crystals of α -PbO and $\text{Pb}_{1-x}(\text{TiO})_x\text{O}$ (typical sizes $0.5 \text{ mm} \times 0.5 \text{ mm} \times 10 \mu\text{m}$) were prepared by hydrothermal synthesis. X-ray-diffraction studies were performed using a two-axis goniometer with Bragg-Brentano geometry with $\text{Cu } K\alpha$ or $\text{Cu } K\beta$ monochromatic radiation from a 18 kW Rigaku rotating anode. The neutron experiments were performed at the Laboratoire Léon Brillouin using the Orphe reactor facilities (Scalay, France) with the two-axis goniometer 3T2 ($\lambda=1.26 \text{ \AA}$) and the 4F2 triple-axis spectrometers ($\lambda=2.662 \text{ \AA}$). In each case for the low-temperature experiments a He cryostat (x ray) or displax refrigerator (neutron) with thermal stability of 0.1 K and precision within 1 K was used. The electron microscopy (TEM) study was performed on a Philips C1120.

III. EXPERIMENTAL RESULTS

A. Precursor effects

TEM diffraction photographs have been performed on α -PbO at room temperature in the $[001]$ zone axis (Fig. 2). Consistently with the $P4/nmm$ symmetry only the reflections with $h+k=2n$ are observed. In addition, strong diffuse scattering around these basic spots is observed in the form of crosses along the $[110]_t^*$ and $[1-10]_t^*$ direction. This diffuse intensity has been studied in the (a^*, b^*) plane by analyzing the diffraction photographs with a microdensitometer. The analysis along the $[110]_t^*$ direction (Fig. 2) reveals that the maximum of the diffuse intensity appears at the two equivalent positions $\pm 0.185(a_t^* + b_t^*)$ from each Bragg peaks. These correspond to positions where the satellite spots appear at lower temperature. Examination perpendicularly to the $[\zeta\zeta 0]^*$ line at various points reveals a constant width $0.0175(a_t^* + b_t^*)$, with the same value as for the Bragg peaks. Extension of the diffuse scattering outside the (a^*, b^*) plane has been analyzed by taking diffraction pho-

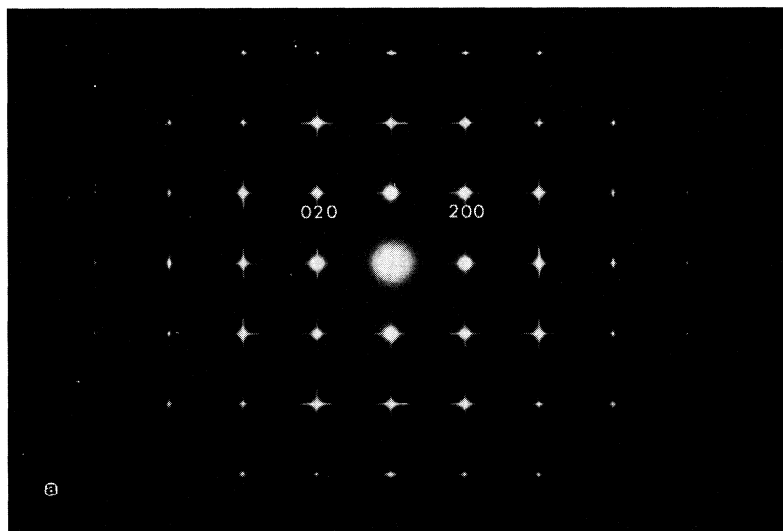
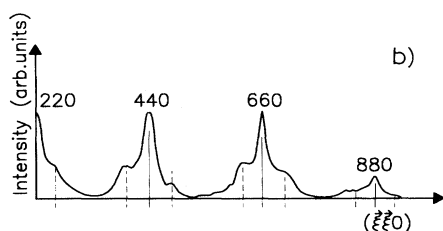


FIG. 2. Room-temperature TEM photograph of the (a^*, b^*) tetragonal plane of α -PbO and microdensitometric measurements along the $[110]_t^*$ direction (notice that the Bragg peaks are saturated). Dashed lines are the locations where satellite spots appear at lower temperature.



tographs with an increasing angle of disorientation, in planes with axial zones $[11-2]_t$ and $[11-3]_t$ [i.e., in $(1-10)_t^*$, $(111)_t^*$ and $(1-10)_t^*$, $(332)_t^*$ planes]: the diffuse intensity has also a component along the $[001]^*$ direction but with an extension smaller than that along the $[110]_t^*$ and $[1-10]_t^*$ directions. This leads to the conclusion that the diffuse intensity along $[110]_t^*$ for instance is roughly ellipsoid shaped with the major axis along $[110]_t^*$ and the two other minor axis along the $[1-10]_t^*$ and $[001]^*$ directions.

Strong oscillations in the background intensity of neutron powder-diffraction patterns have already been reported.² It was noticed that these oscillations disappear below the critical temperature T_I and it was suggested that they constitute dynamical pretransitional effects of the phase transition. In order to settle this assertion we have performed a more detailed study and analysis of this phenomenon and have correlated it to the TEM study.

In a first step we have recorded between 720 and 8 K full neutron-diffraction patterns from which we have extracted the background. Figure 3 shows some patterns at different temperatures: it reveals strong oscillations at high temperature approximately centered at $2 \sin \Theta / \lambda \approx 0.6, 0.9$, and 1.1 \AA^{-1} in addition to the classical thermal component due to thermal agitation. When cooling, these oscillations strongly diminish, however they do not completely disappear below T_I and get no further appreciable thermal evolution: down to at least 8 K small oscillations are still detected.

These oscillations in the powder-diffraction patterns could be correlated to the TEM observations of diffuse scattering described above. Indeed these oscillations can qualitatively

be reproduced by integrating the diffuse intensities in the TEM photographs obtained from microdensitometry: this integration has revealed maximum at $\approx 0.6, 0.9$, and 1.1 \AA^{-1}

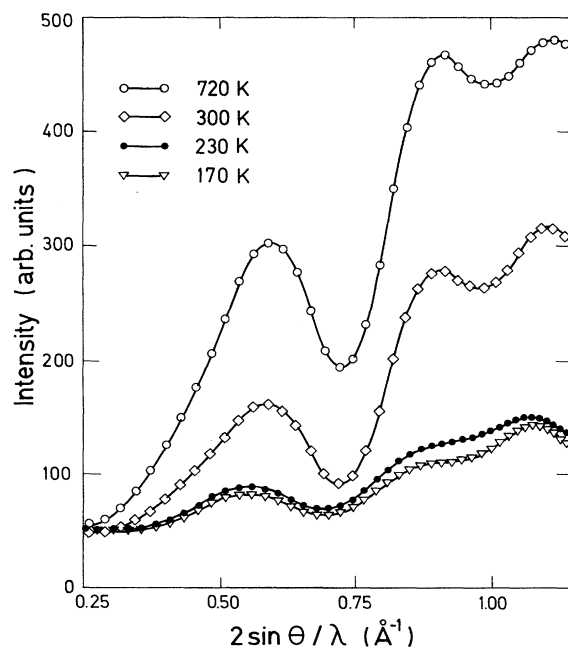


FIG. 3. Diffuse scattering observed as background's oscillations in neutron-diffraction two-axis experiments versus temperature on α -PbO; the Bragg peaks have been removed.

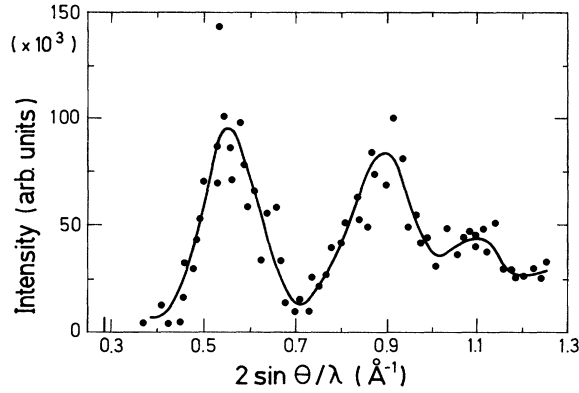


FIG. 4. Diffuse scattering calculated by integration of the diffuse scattering measured in TEM experiment on α -PbO (see Fig. 2). The solid line is a guide for the eyes.

(Fig. 4). Clearly the oscillations in the neutron patterns and the diffuse scattering in the TEM photographs are the manifestation of the same phenomenon.

In a second step, triple-axis experiments were performed on powdered samples. An energy analysis of the first oscillation in the diffraction patterns at $q=0.6 \text{ \AA}^{-1}$ was achieved by recording patterns at different energy transfers, between 0 and 1000 Ghz. This experiment reveals that the oscillations of the scattering background in the double-axis type of experiments where all energies are integrated has a dynamic origin. For 700 Ghz transfer energy we have observed the same oscillations of the scattering as in the energy-integrated experiments, whereas for the elastic measurement with the triple-axis setup at zero transfer energy, we were not able to reproduce significant oscillation of the background (Fig. 5).

While no low-temperature phase transition occurs in both compounds SnO and $\text{Pb}_{1-x}(\text{TiO})_x\text{O}$, strong diffuse scattering in the background of the neutron powder-diffraction patterns at room temperature and down to 6 K is evidenced. In $\text{PbO}_{(1-x)}(\text{TiO})_x\text{O}$ it has approximately the same intensity as for PbO, but is weaker in SnO. The TEM experiments show that this diffuse scattering is along the same directions as for α -PbO ($[110]_t^*$ and $[1-10]_t^*$) but is centered at $q=0$ and does not possess any maxima near $q=\delta$ (Fig. 6). When cooling, this diffuse scattering seems to diminish only slightly and is still observed at 8 K.

B. Phase transition

Below the critical temperature T_I the tetragonal symmetry of α -PbO is broken as the average lattice of the incommensurate phase is orthorhombic. This shows up in the results of a weak temperature-dependent distortion. The thermal evolution of the corresponding lattice parameters was already reported.² Here, we present a Debye analysis of these evolutions (Fig. 7) with the classical law

$$p = p_0 + 9ART(T/\Theta_D)^3 \int_0^{\Theta_D/T} \frac{t^3 dt}{e^t - 1},$$

where p_0 is the lattice parameter at 0 K and Θ_D is the Debye temperature, R is the universal gas constant, and A is a multiplicative coefficient. So the three coefficients p_0 , Θ_D , and A are the fitting parameters.

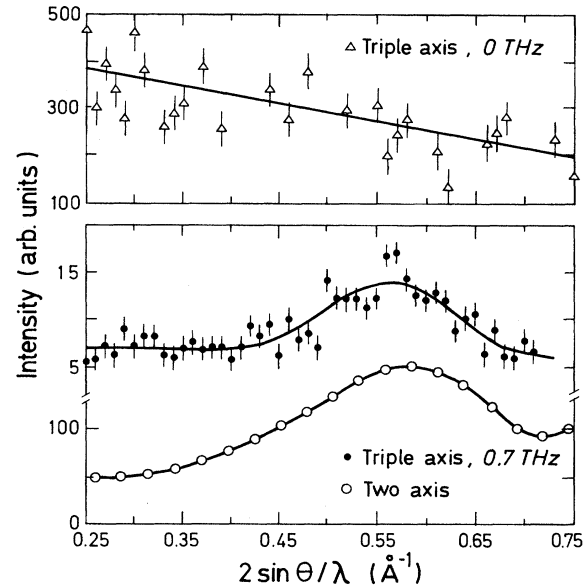


FIG. 5. Diffuse scattering observed by triple-axis spectrometer measurement (0 and 0.7 THz) compared with a measurement (from Fig. 3) on a two-axis spectrometer. The solid lines are a guide for the eyes.

In lead oxide the thermal evolution of the c parameter displays no anomaly at T_I and could be fitted in the whole range of temperature (6–600 K) by a single evolution whereas the evolutions of a_0 and b_0 below T_I are distinct from that of $a_t\sqrt{2}$ above T_I . The values of Debye temperatures reveal the weak rigidity of the bondings in the c direction ($\Theta_D=77 \text{ K}$) in contrast with those in the a, b plane ($\Theta_D=570 \text{ K}$). This anisotropy is also revealed by the different values in the thermal dilatation at 300 K ($\alpha_c=24 \times 10^{-6} \text{ K}^{-1}$ and $\alpha_a=15 \times 10^{-6} \text{ K}^{-1}$).

The spontaneous strain ε_{12} was deduced from the thermal evolution of the a_0 and b_0 parameters; a power law

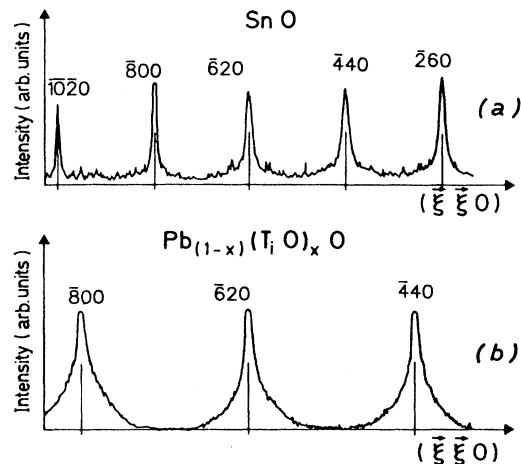


FIG. 6. Microdensitometric measurements along $[110]_t^*$, direction of TEM photographs of the (a^*, b^*) tetragonal plane at room temperature for SnO and $\text{Pb}_{(1-x)}(\text{TiO})_x\text{O}$ (notice that the Bragg peaks are saturated).

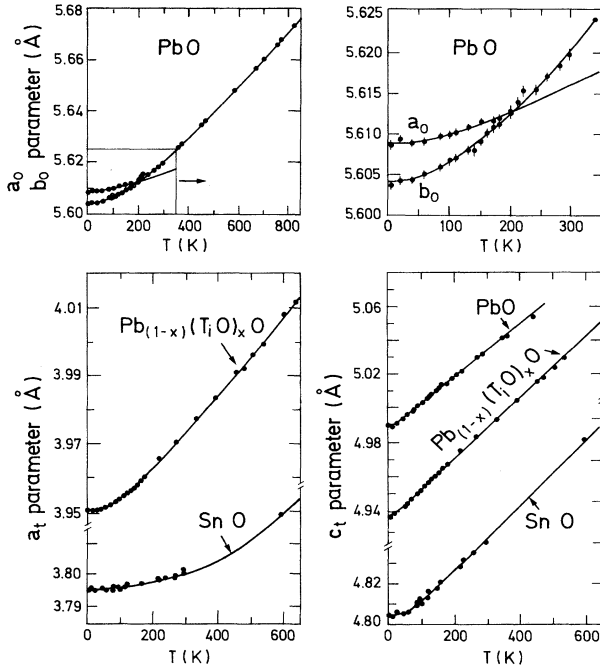


FIG. 7. Thermal evolutions of the tetragonal lattice parameters in α -PbO, SnO, and $\text{PbO}_{(1-x)}(\text{TiO})_x\text{O}$. The solid lines are fitted by Debye evolutions.

$B(T_I - T)^m$ was fitted and gives $m=0.77(2)$ and $T_I=227(1)$ K. These values are very different from those reported by Boher and Garnier⁹ ($m=0.5$ and $T_I=200$ K) and it is probably due to the lack of data above 180 K. The high m value suggests that the spontaneous strain could be a secondary order parameter. Comparison with the evolution of the satellite intensity versus temperature will demonstrate this point (see below).

While isotopic compounds SnO and $\text{PbO}_{(1-x)}(\text{TiO})_x\text{O}$ do not possess low-temperature phase transition, as no distortion of the tetragonal phase as well as no satellite peaks are evidenced by any diffraction techniques, it is interesting to compare the thermal evolutions of their lattice parameters a and c (Fig. 7) with those of PbO.

At room temperature the lattice parameters in PbO are 3.9777 and 5.0259 Å ($c/a=1.2635$) and the introduction of TiO_2 induces a contraction of the tetragonal cell parameters $a=3.9665$ Å and $c=4.9831$ Å ($c/a=1.2563$) which is more important perpendicularly to the layer of Pb atoms than in the layer ($\Delta c/c=0.85\%$ and $\Delta a/a=0.28\%$). The room-temperature lattice parameters of SnO are $a=3.8012$ Å and $c=4.8393$ Å ($c/a=1.2731$).

The thermal evolutions of both compound SnO and $\text{PbO}_{(1-x)}(\text{TiO})_x\text{O}$ were satisfactorily fitted with a Debye law in the whole range of temperature (6–600 K) (Fig. 7). Considering $\text{PbO}_{(1-x)}(\text{TiO})_x\text{O}$, the Debye temperature and the thermal dilatation parameter α at 300 K are about the same as in lead oxide. SnO, however, possesses higher Debye temperatures revealing stronger rigidity of bonding; besides the higher value of α_c indicates weaker bonding in this direction.

In lead oxide PbO, experiments below T_I by TEM show the appearance of satellite peaks in the $[110]_t$ and $[1-10]_t$ directions (Fig. 8) in agreement with the x-ray precession results by Moreau *et al.*:² the occurrence of satellite peaks in both directions was explained by the coexistence of the two types of orthorhombic domains. In this study we have observed high-order satellite peaks (up to 3) with typical values of intensity equal to 10 and 1 % for second- and third-order relatively to the first-order peaks. Moreover, coherently with the neutron-diffraction experiments, a small component of diffuse scattering persists at low temperature.

We have performed a study of the satellite and Bragg peaks using high resolution x-ray powder diffraction. We found in agreement with previous reported value² $\delta=0.370(3)b_0^*$ in the whole range of study (6 K– T_I) for samples with different purities and different preparations. Fitting of the evolutions of the satellite peaks intensity 3111 and 311-1 with a power law $I=I_0(T_I-T)^{-2\beta}$ gives $\beta=0.36(2)$ and $T_I=227(1)$ K coherently with the values obtained by fitting the spontaneous strain ε_{12} evolution. This experimental value of β corresponds to Wilson theoretical value of 0.3645 for three-dimensional systems and two-dimensional order parameters.

C. Structural study

Structural evolution of the prototype and incommensurate phase of α -PbO by neutron and x-ray powder refinements using the full patterns (Bragg and satellite peaks) has already been reported,⁵ as well as the structural evolution of $\text{PbO}_{(1-x)}(\text{TiO})_x\text{O}$ (Ref. 7) from room temperature down to 8 K. In PbO and $\text{PbO}_{(1-x)}(\text{TiO})_x\text{O}$ data at some interesting temperatures were lacking so we have completed these informations by making new neutron and x-ray experiments and have (re)analyzed the whole set of data. On the other hand, no information exists below room temperature for tin oxide SnO and we have performed a complete data collection from room temperature down to 8 K.

As it has been pointed out above, the room-temperature structure of α -PbO is a very simple layered structure with only one structural parameter, i.e., the z coordinate of the lead atoms. The cell is tetragonal with a $P4/nmm$ space group ($Z=2$). The oxygen atoms form a square lattice and the lead atoms are at the vertexes of pyramids with these four basal oxygen atoms (Fig. 1). The layers of lead atoms (2.37 Å) are separated by large interlayers (2.66 Å) which are only occupied by the lone pairs; the bonding lengths Pb-O and O-O are at room temperature 2.31 and 2.81 Å, respectively.

Introduction of TiO_2 forms a solid solution $\text{PbO}_{(1-x)}(\text{TiO})_x\text{O}$ for $x=4.5$ to 8 % with the litharge structure where Ti^{4+} ions substitute for the Pb^{2+} ions and the extra oxygen atom for the electronic lone pairs in the interlayer of the PbO host lattice structure (Fig. 1). At room temperature the layer, interlayer, and Pb-O, O-O distances are 2.38, 2.59, 2.31, and 2.80 Å, respectively. The enhancement of anisotropy compared with α -PbO which has been noticed in the lattice parameters measurement (Sec. III B) is due to the presence of the extra oxygen atom in the interlayer which creates new interlayer Pb-O (3.13 Å) and Ti-O (1.78 Å) bonds.

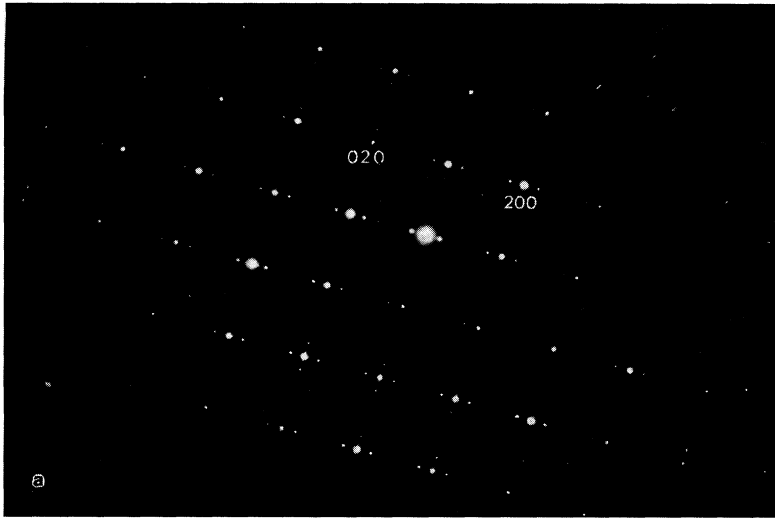
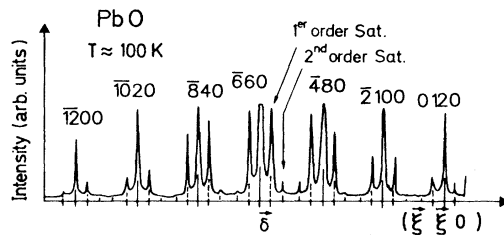


FIG. 8. TEM photograph ($T \approx 100$ K) of the (a^*, b^*) tetragonal plane of α -PbO and microdensitometric measurements along the $[110]_t^*$ direction in the incommensurate phase of α -PbO (notice that the Bragg peaks are saturated). First- and second-order satellite peaks are observed.



At room temperature the structural refinement of SnO reveals the greater compactness of its structure observed in the lattice parameters measurement, compared with those of α -PbO and $\text{PbO}_{(1-x)}(\text{TiO})_x\text{O}$. Indeed the layer, interlayer and Sn-O, O-O distances are shorter (2.29, 2.55, 2.22, and 2.69 Å), respectively, at room temperature, than the corresponding distances in the two other compounds.

Regarding the structural evolutions of SnO and $\text{PbO}_{(1-x)}(\text{TiO})_x\text{O}$ and of the average structure of PbO, one interesting result is the fact that the thermal expansion in the c direction is essentially due to the thermal expansion of the interlayer distance (Fig. 9), the layer distance being almost temperature independent. The higher value for α in tin oxide interlayers indicates weaker interactions inside the interlayer than for the two other compounds. The thermal evolutions of bonding lengths (Fig. 10) show that the Pb-O distances are almost equivalent in PbO and $\text{PbO}_{(1-x)}(\text{TiO})_x\text{O}$ and the Sn-O distance gets smaller values but with similar evolution.

Comparison⁵ of the average and prototype structure with the incommensurate structure of PbO show that this latter phase results from small displacements from the prototype phase, for both types of atoms mainly in the a_0, b_0 plane with a typical modulation amplitude value equal to 0.15 Å. This structure is analyzed in Sec. IV.

IV. LONE PAIRS LOCALIZATION AND ELECTROSTATIC ENERGY CALCULATION

A. Method

We have recently reported a method which allows us to localize the electronic lone pairs of a given structure.¹⁰ In

this method we consider an infinite ionic crystal with spherical nonrecovering charges distribution and the lone pairs are approximated to point charges. The ions possessing a lone pair are then formed of a relative charge $N+2$, N being the charge of the ion located at the atomic position, and a relative charge -2 at the lone pair's position. Thus the electric dipolar momentum of an ion possessing a lone pair is equal to $q\zeta$, q being the electric charge of a lone pair, i.e., $-2|e|$, and ζ being the vector that links the nucleus of the ion to the center of its associated lone pair ζ is thus a measure of the extension of the lone pair in the structure. The relation between the ζ vector and the local electric field \mathbf{E} is then

$$q\zeta = \alpha\mathbf{E}, \quad (1)$$

α being the electronic polarizability of the ion which has a lone pair. The electric local field is assumed to be constant between the nucleus and the lone pair so that it can be taken on the position of the nucleus.

Starting with the knowledge of the structural data and of the electronic polarizability α (respectively equal to 4.9 and 4.0 Å³ for the Pb^{2+} and Sn^{2+} ions) the determination of the equilibrium in Eq. (1) is made by an iteration process. In a first step the calculation of the local electric field \mathbf{E} on the different ions of the unit cell possessing a lone pair is performed using Ewald's method¹¹ adapted by Verbaere, Marchand, and Tournoux.¹² This first calculation is made with arbitrary positions of the lone pairs, for instance, centered on the nucleus by taking $\zeta=0$. Then the position of each lone

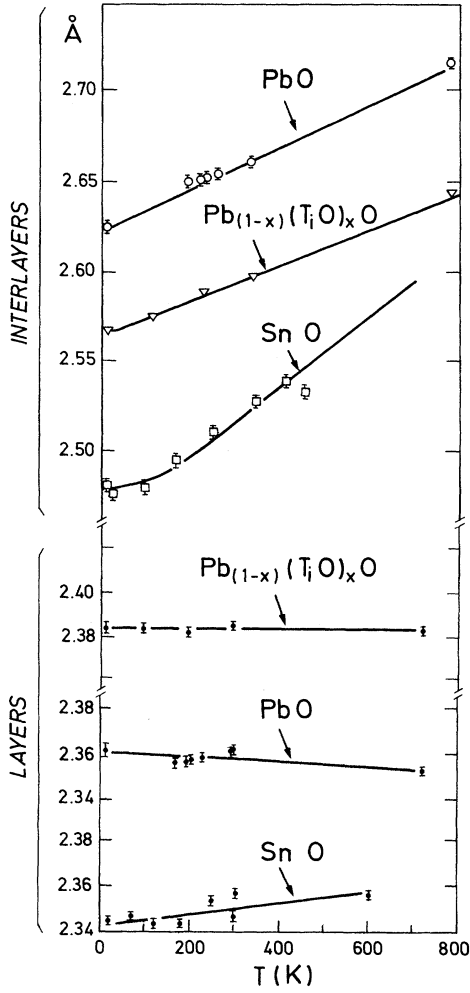


FIG. 9. Thermal evolution of the layer and interlayer distances (see Fig. 1) in the structures of α -PbO, SnO, and $\text{PbO}_{(1-x)}(\text{TiO})_x\text{O}$.

pair is modified according to Eq. (1). But as that modification of position implies a modification of the local electric fields \mathbf{E} , the calculation is repeated until the equilibrium between electric dipoles $\boldsymbol{\zeta}$ and local electric fields \mathbf{E} is achieved. So this method takes into account not only the ions of the structure, but also the electrostatic influence of the lone pairs.

Then the energy of the resulting structure is calculated, the lone pairs being considered as ions with $-2|e|$ charges. The total energy (also called the cohesion energy corresponding to the opposite of the sublimation energy) includes the electrostatic energy of the ionic structure which can be written as

$$W_{\text{el}} = 1/2 \sum_{p,p'} \sum_{\mathbf{h}} z_p z_{p'} |e|^2 / t$$

with $t = |\mathbf{r}'_p - \mathbf{r}_h - \mathbf{r}_p|$ and p and p' being the indexes of the unit-cell ions, \mathbf{h} indexing the crystal cells, and $z_p |e|, z_{p'} |e|$ are the charges of the p and p' ions (the prime on the second summation means that the case $h_1 = h_2 = h_3 = 0$ is excluded

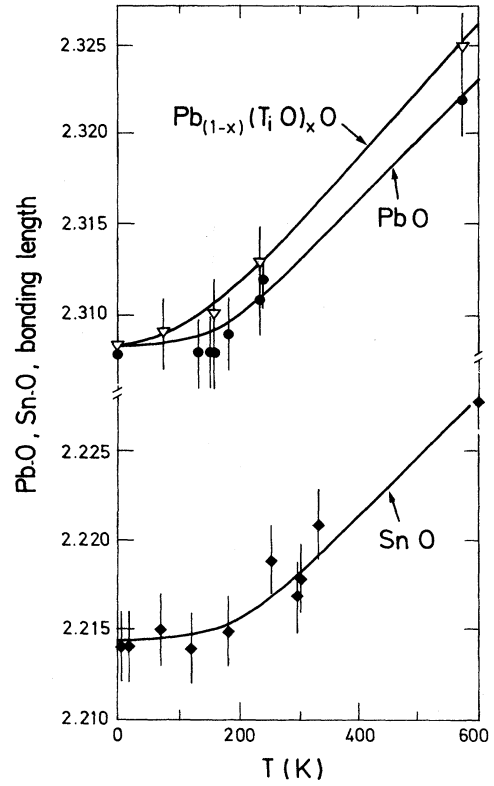


FIG. 10. Thermal evolution of the Pb-O and Sn-O bonding lengths in α -PbO, SnO, and $\text{PbO}_{(1-x)}(\text{TiO})_x\text{O}$.

when $p = p'$). Another part of the (total) cohesion energy is the energy of creation of the lone pairs. It corresponds to the energy needed to divide the ions into two charges: the nucleus-centered charge and the lone pair, i.e., the energy needed for the polarization of the ions. Thus this energy can be approximated by the creation energy of the dipole corresponding to the two charges, i.e.,

$$W_{\text{cre}} = 1/2 \sum \boldsymbol{\mu}_p \cdot \mathbf{E}_p^{\text{loc}},$$

p being the index of the lone pairs, $\boldsymbol{\mu}_p = z_p \boldsymbol{\zeta}_p$. This is an approximation as the distance $|\boldsymbol{\zeta}_p|$ between the nucleus and its lone pair is not negligible.

To those Coulomb-type energies should be added a repulsive Pauli-type energy W_{rep} . Because of its abrupt shape, this repulsive energy *at the equilibrium position*, is very small in comparison with the attractive electrostatic energy which then is the main component of the energy of cohesion and can be neglected. We have also neglected the ionization energies appearing in the transformation of the neutral atoms to ions which is only an additive constant in the structural changes that we have considered here.

B. Results

In the room-temperature tetragonal phases of PbO and SnO and in the low-temperature phases of SnO (tetragonal) and PbO (orthorhombic average lattice) the direction of the lone pairs L ($\boldsymbol{\zeta} = \text{Pb}-L$, where Pb is the position of the lead

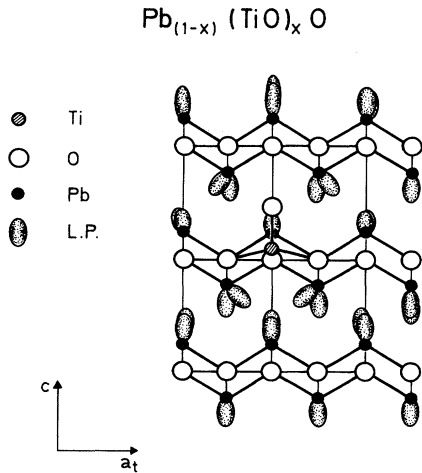


FIG. 11. Lone pairs localization in the room-temperature structure of $\text{PbO}_{(1-x)}(\text{TiO})_x\text{O}$.

ion) is along the c axis because of the symmetry of the lead atoms site. In PbO we have calculated a distance $|\zeta| = 0.995 \text{ \AA}$ at 300 K and a shorter distance 0.903 \AA in SnO ; when cooling down to 8 K both values of $|\zeta|$ increase up to 1.008 and 0.911 \AA , respectively.

The influence of the substitution of a lead atom-lone pair group by a TiO group on the neighboring lone pairs has been studied at 8 K. Important tiltings up to 12.9° are observed (Fig. 11) as well as large variation in the $|\zeta|$ value from 0.94 to 1.12 \AA ; above the tenth neighbor the influence of the Ti atom becomes negligible. The average length $|\zeta|$ is 1.003 \AA , i.e., almost the same as in PbO at the same temperature (1.008 \AA).

We have calculated the lone pairs localization inside the incommensurate phase of PbO using the modulated displacement from Hedoux, Grebille, and Garnier⁵ (notice the change of origin), i.e.,

$$\begin{aligned} &\text{for Pb } (0.25, 0.25, z = -0.2367) \\ &u_x = 0.023 \cos[2\pi\delta(y - y_0)], \\ &u_y = 0.024 \sin[2\pi\delta(y - y_0)], \\ &u_z = 0.019 \cos[2\pi\delta(y - y_0)], \end{aligned} \quad (2)$$

and

$$\begin{aligned} &\text{for O } (0, 0, 0) \quad u_x = 0.013 \cos[2\pi\delta(y - y_0)], \\ &u_y = 0.012 \sin[2\pi\delta(y - y_0)], \\ &u_z = -0.008 \sin[2\pi\delta(y - y_0)]. \end{aligned}$$

The resulting representation (Fig. 12) shows a more complex modulation than expected on the basis of simple stereochemical considerations. One principally notices the tilting of the lone pairs in the direction of the displacement of the oxygen atoms. The distance between lone pairs ($L-L$) is practically not modified on average (2.87 \AA), compared with the non-modulated case; however the distance between the oxygen

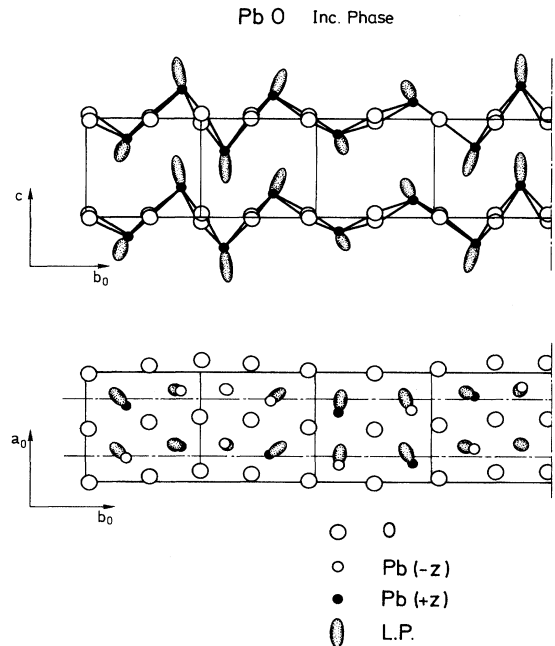


FIG. 12. Incommensurate structure of $\alpha\text{-PbO}$ with the lone pairs localization. Amplitudes of modulation have been magnified by a factor 5.

atom and the lone pair ($O-L$) and the extensions ζ are increased on average: the modulation allows a greater extension of the lone pairs while keeping an unchanged $L-L$ distance.

The difference of electrostatic energy per chemical formula between the incommensurate phase and the nonmodulated (average) phase of lead oxide has been calculated for different values of the misfit parameter δ , taking into account the calculated positions of the lone pairs. In a first step the modulation amplitudes were kept constant and the misfit parameter δ was changed. The results show (Fig. 13) that the energy of the modulated structure is minimized for a value of $\delta_{\text{cal}} \approx 0.31$ which is to be compared to the experimental value 0.370 . Changing the amplitudes modulations only leads to a change of unit in the energy in Fig. 13 as the (relative) energy is proportional to the square of these amplitudes and does not affect the shape of the curve. On the contrary, changing the α polarizability coefficient strongly affects the δ dependence of the energy: decreasing the α value from 4.9 to zero induces the vanishing of the minimum at δ_{cal} for $\alpha = 2.0 \text{ \AA}^3$. As the extension of the lone pair is directly related to the electronic polarizability this result points out the connection of the instability at δ to the existence of these lone pairs.

In the same spirit we have used the structural data of SnO and introduced an hypothetical modulation similar to that of lead oxide. The evolution is drastically different as no minimum in the curve (Fig. 13) appears. Changing the value of α for Sn from 4.0 to the same value as for Pb, i.e., 4.9 \AA^3 restore a minimum in the curve at $\delta_{\text{cal}} \approx 0.31$, pointing out again the importance of the extension of the lone pair for the existence or absence of instability in the structure.

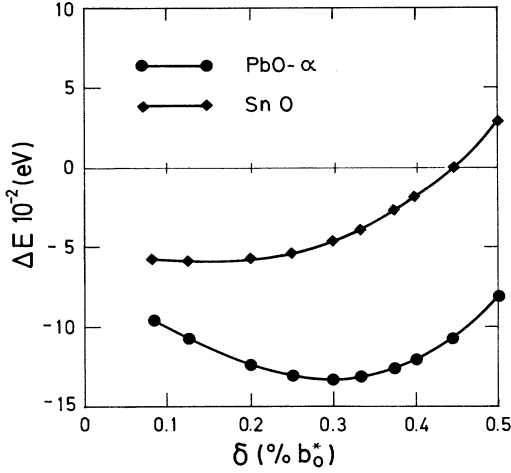


FIG. 13. Variation of electrostatic energy (per chemical formula) between the incommensurate phase and the average phase of α -PbO, and for SnO when imposing an identical (hypothetical) modulation. An instability is observed only in α -PbO at $\delta_{\text{cal}}=0.31$.

A further step in the analysis of the instability was obtained by breaking the global electrostatic energy into its different components. Indeed in the structure of lead oxide, the contribution of the Pb^{2+} and O^{2-} ions and that of the lone pairs which has almost the same role as electric dipoles can be separated: the total energy includes three terms which are the charge-charge Coulomb interactions, the charge-dipole interactions and the dipole-dipole interactions. The first term (charge-charge) was calculated by only introducing the Pb^{2+} and O^{2-} ions (i.e., neglecting the lone pairs), the third term (dipole-dipole) was calculated by introducing only the lone pairs (i.e., neglecting the Pb^{2+} and O^{2-} ions) and the second term was calculated by subtracting from the total energy the first and third terms. The results (Fig. 14) indicate that the dipole-dipole interactions, that is the interactions between lone pairs, are responsible for the minimum of the total energy.

Further we have tried to know which of the components of the modulation are essential for the occurrence of the incommensurate instability. It appears that the components along a_0 are not essential, since the minimum in the electrostatic energy (Fig. 13) is obtained even if only the components of the modulation along the b_0, c plane are introduced.

Finally we have studied the influence of the displacement of a given Pb^{2+} ion (keeping the rest of the structure constant) on the proximate lead neighbors by calculating the induced electrostatic electric field \mathbf{E} on these ions. We have only considered movements inside the b_0, c plane which are the essential ones for the instability as explained just above. In the table we give the components along b_0 and c of the supplementary electric field induced by the movement of an initial lead atom along an ellipse with major and minor axis equal to the amplitudes of modulations [Eqs. (2)] in the corresponding directions for different values of the phase θ on this ellipse. As the electrostatic field is nonzero along the c direction in the average phase (which induces the lone pairs delocalization), we have subtracted this constant value to the

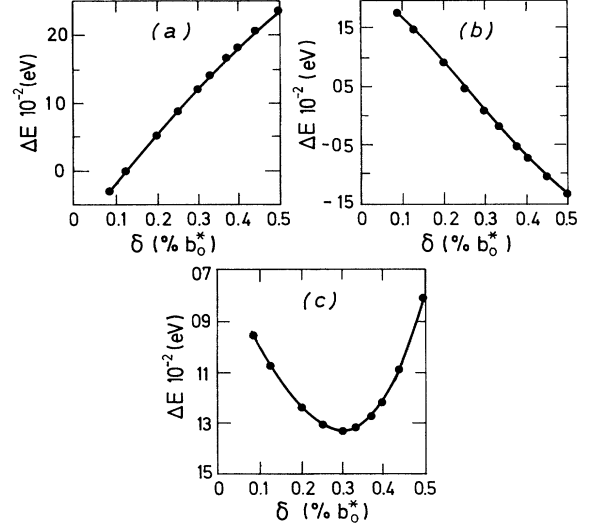


FIG. 14. Different contributions in the electrostatic energy (per chemical formula) between the incommensurate phase and the average phase of α -PbO from Fig. 14(a) Coulomb interactions contribution; (b) Charges-dipole interactions contribution; (c) Dipole-dipoles (i.e., lone pairs-lone pairs) interactions contribution. The minimum in the total energy results from these latter interactions.

calculated electric field, which leads to the ΔE_c values. It can be observed that a given movement of the first Pb^{2+} ion (whose unshifted position is at $00z$) along an ellipse in the b_0, c plane (anticlockwise for instance) induces movements of rotation in the opposite direction (i.e., clockwise) on both the first-neighbor lead atom (close to $0.505 - z$) and second-neighbor lead atom (close to $11z$), i.e., a frustration on the second neighbor is induced. This result, as discussed below, could explain, in a simple pseudospin approximation the stabilization of the incommensurate phase down to 0 K.

V. SUMMARY AND CONCLUSIONS

In this study we have discussed the main features of the incommensurate phase of α -PbO using a combination of x-ray, neutron, and TEM diffraction and diffusion, and calculations with simple ionic approximations. In summary an incommensurate modulation appears in the tetragonal phase of α -PbO below $T_I=227$ K, with a single q along in the $[110]_t$ direction with a misfit vector $\delta=0.370(e)\mathbf{b}_0^*$ which is temperature and sample independent, and a critical exponent $\beta=0.36(1)$. This modulation breaks the tetragonal symmetry and the average symmetry of the incommensurate phase is orthorhombic with $\mathbf{a}_0=\mathbf{a}_t+\mathbf{b}_t$ and $\mathbf{b}_0=\mathbf{a}_t-\mathbf{b}_t$ and $\mathbf{c}_0=\mathbf{c}_t$; the ferroelastic distortion ε_{12} is a secondary order parameter with a temperature dependence with a $\approx 2\beta$ exponent. Strong diffuse scattering intensity in the direction of the modulation and centered at $\mathbf{Q}=\delta$ is observed at room temperature; this intensity seems to be essentially dynamical and almost disappears below T_I ; however a small static part remains down to 8 K. Structural refinements of the incommensurate phase indicate that the modulated structure results

TABLE I. Results of calculations of electric field on first or second neighboring lead atoms when a lead atom is shifted in the b_0 , c plane along an ellipse with major and minor axis equal to the amplitude of modulations [Eqs. (2)]; θ is the phase angle along this ellipse. E_b and ΔE_c are the components of the electric field along the b_0 and c orthorhombic axis.

Positions of the initial lead atom	First neighbor		Second neighbor	
	E_b ($e \text{ \AA}^{-2}$)	ΔE_c ($e \text{ \AA}^{-2}$)	E_b ($e \text{ \AA}^{-2}$)	ΔE_c ($e \text{ \AA}^{-2}$)
$\theta=0$	-0.0038	-0.0107	0.0056	-0.0001
$\theta=\pi/4$	-0.0059	-0.0001	0.0039	-0.0004
$\theta=\pi/2$	-0.0041	0.0095	0.0000	-0.0024
$\theta=\pi$	0.0021	0.0097	-0.0055	-0.0063
$\theta=3\pi/2$	0.0045	-0.0081	0.0000	-0.0001
$\theta=7\pi/4$	0.0012	-0.0142	0.0039	0.0001

from small displacements of both lead and oxygen atoms from their high-temperature positions. So the experimental results seem to indicate a physical picture of the transition which is in a first approximation of the displacive type, induced by the softening of a lattice-phonon mode.

Isotypic compounds $\text{PbO}_{(1-x)}(\text{TiO})_x\text{O}$ and SnO reveal at room temperature diffuse scattering intensity along the same direction as in lead oxide but centered in $\mathbf{Q}=0$. However only weak thermal evolution of this intensity is observed when cooling and no satellite peak, as well as no distortion appears at low temperature.

The main structural difference between PbO and $\text{PbO}_{(1-x)}(\text{TiO})_x\text{O}$ is the introduction inside the layer of a supplementary oxygen atom. As interactions between the lone pairs of the lead atoms are supposed to be responsible for the existence of the phase transition, this suggests that the introduction of a supplementary oxygen atom modifies these interactions and leads to the disappearance of the phase transition. In SnO the main structural difference with lead oxide is the lower value of the interlayer distance, which could result from smaller extension of the electronic lone pairs and thus a decreasing of the interactions responsible for the transition. Of course at this stage these ideas are purely speculative; however model calculations support more strongly these assertions.

Indeed using a simple ionic approximation we have performed the localization of the lone pairs inside the structures of the three isotypic compounds. A higher extension ζ of the lone pairs in $\alpha\text{-PbO}$ is observed compared to SnO and $\text{PbO}_{(1-x)}(\text{TiO})_x\text{O}$; introduction of TiO induces locally strong tilting of these lone pairs from the fourfold axis. Moreover the low-temperature modulation allows the L - L distances to increase inside the incommensurate phase without changing their extension: the steric occupancy of the lone pairs is in a sense "optimized" by the appearance of the incommensurate phase.

The study of Coulomb interactions shows unstable positions of Pb^{2+} and O^{2-} from an electrostatic point of view, which results in an energy minimum along the $[110]_l$ direction at a position $\delta \approx 0.31$ close to the experimental value of 0.375, the difference being most probably due to the fact that the covalent part of the bonding are neglected in the calculation. This instability is due to the dipole-dipole (i.e., lone pair-lone pair) interactions. Moreover this instability disap-

pears when the polarizability of the ion diminishes, which is physically realized in SnO . Probably in $\text{PbO}_{(1-x)}(\text{TiO})_x\text{O}$ the local perturbations induced by the additional oxygen atom inside the interlayers creates a kind of "screening" of the interactions which are responsible for the phase transition in lead oxide.

Benkert, Heine, and Simmons¹³ have shown the possibility of stabilizing an incommensurate phase down to 0 K through a pseudospin model of the anisotropic next-nearest-neighbor Ising type that they successfully apply to ThBr_4 and biphenyl, although the dipolar and elastic forces are long range. In this model the pseudospin is a rotation or a torsion of atomic groups of the structure and can continuously change from -1 to $+1$ inside a double-well potential. In that case the stability of the incommensurate phase down to 0 K implies a ferromagneticlike coupling ($J_0 > 0$) between different chains of pseudospins, a positive or negative coupling ($J_1 < 0$ or $J_1 > 0$) between nearest neighbors in the chain direction, and an "antiferromagnetic" coupling between second neighbors ($J_2 > 0$), and the condition $J_1/4J_2 < 1$.

We have tried to check such a condition in PbO in order to explain the absence of lock-in transition at low temperature. Defining pseudospins as the angles of rotation of the Pb atoms around their equilibrium positions we make use of the results of Sec. IV. As the energy associated to a displacement of a charge inside a uniform field is proportional to the intensity of this field we can deduce using Table I the ratio of couplings between the first neighbors and of the second neighbors $J_1/4J_2$ from the ratio of the average electric field $\langle |\Delta \mathbf{E}| \rangle$, where the spatial average $\langle \rangle$ is made on the positions from $\theta=0$ to $\theta=2\pi$. We find for first neighbor $\langle |\Delta \mathbf{E}| \rangle = 0.00102 \text{ \AA}^{-2}$ and for second neighbor $\langle |\Delta \mathbf{E}| \rangle = 0.00036 \text{ \AA}^{-2}$, which leads to a ratio of 0.7. Thus we believe from the Benkert model that the stability of the incommensurate phase down to the lowest temperatures is due to a frustration on the second neighbors arising from electrostatic interactions.

However, many features of the mechanism of the incommensurate phase remain unclear. In particular the origin of the diffuse scattering in SnO and $\text{PbO}_{(1-x)}(\text{TiO})_x\text{O}$, as well as the low-temperature contribution observed in PbO is not understood. In order to get deeper insight of this problem inelastic neutron-scattering study should be done if samples

of sufficient size could be grown. Moreover the structure of the modulated phase is still not perfectly understood; in particular a recent study by Withers and Schmid¹⁴ using TEM indicate (P_{s-11}^{Cmma}) as the space group in contradiction with

our space-group determination (P_{-1-11}^{C2mb}). However we believe that this problem should imply a four-circles study, which up to now has failed, as single crystals of sufficient size are still lacking.

* Author to whom correspondence should be addressed.

¹D. M. Adams, A. G. Christy, J. Haines, and S. M. Clark, *Phys. Rev. B* **46**, 11 358 (1992).

²J. Moreau, J. M. Kiat, P. Garnier, and G. Calvarin, *Phys. Rev. B* **39**, 10 296 (1989).

³J. R. Schoonover, T. L. Groy, and S. H. Lin, *J. Solid State Chem.* **83**, 207 (1989); J. R. Schoonover, *ibid.* **100**, 331 (1992).

⁴J. Galy, G. Meunier, S. Andersson, and A. Åström, *J. Solid State Chem.* **13**, 142 (1975).

⁵A. Hédoux, D. Grebille, and P. Garnier, *Phys. Rev. B* **40**, 10 653 (1989).

⁶K. Oka, H. Unoki, and T. Sakudo, *J. Cryst. Growth* **47**, 568 (1979).

⁷J. Moreau, P. Boher, and P. Garnier, *Mater. Res. Bull.* **24**, 1241 (1989).

⁸D. LeBellac, J. M. Kiat, A. Hédoux, P. Garnier, D. Grebille, Y. Guinet, and I. Noiret, *Ferroelectrics* **125**, 215 (1992); D. LeBellac, PhD. thesis, Université d'Orsay, 1993.

⁹P. Boher and P. Garnier, *C. R. Acad. Sci. Série II* **298**, 203 (1984).

¹⁰D. LeBellac, J. M. Kiat, and P. Garnier, *J. Solid State Chem.* **114**, 459 (1995).

¹¹M. P. Tosi, in *Solid State Phys.: Advances in Research and Applications* (Academic, New York, 1974), Vol. 16, p. 1.

¹²A. Verbaere, R. Marchand, and M. Tournoux, *J. Solid State Chem.* **23**, 383 (1978).

¹³C. Benkert, V. Heine, and E. H. Simmons, *Europhys. Lett.* **3**, 833 (1987).

¹⁴R. L. Withers and S. Schmid, *J. Solid State Chem.* **113**, 272 (1994).

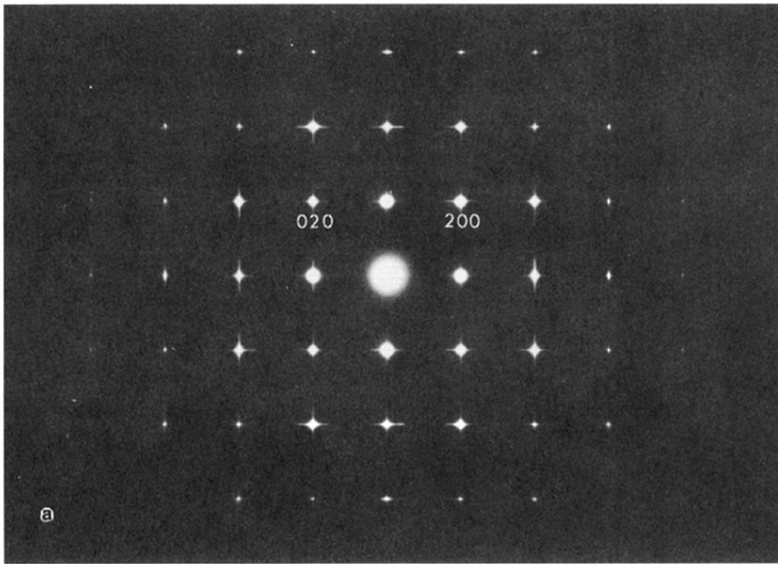
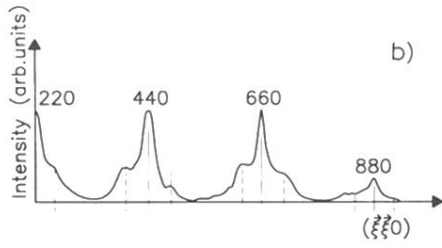


FIG. 2. Room-temperature TEM photograph of the (a^*, b^*) tetragonal plane of α -PbO and microdensitometric measurements along the $[110]t^*$ direction (notice that the Bragg peaks are saturated). Dashed lines are the locations where satellite spots appear at lower temperature.



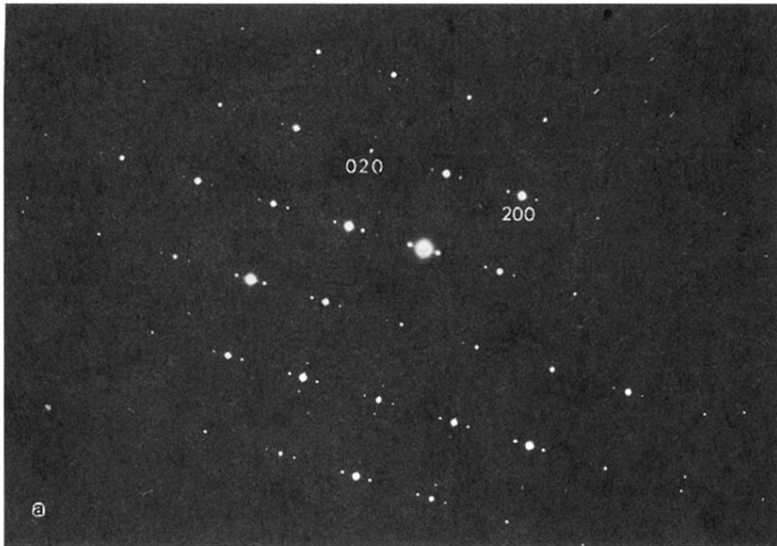


FIG. 8. TEM photograph ($T \approx 100$ K) of the (a^*, b^*) tetragonal plane of α -PbO and microdensitometric measurements along the $[110]_t^*$ direction in the incommensurate phase of α -PbO (notice that the Bragg peaks are saturated). First- and second-order satellite peaks are observed.

